deepthought: domain driven design for microscopy with applications in DNA damage responses

P. S. Kesavan[1,3]✉ **and Darshika Bohra**[2]

[1]NDimensional Systems
[2]Tata Institute of Fundamental Research, Hyderabad, India
[3]Work done at: Tata Institute of Fundamental Research, Hyderabad, India

Microscope systems have traditionally separated data acquisition and analysis into distinct phases, limiting real-time insights and experimental adaptability. While open-source tools exist for device control, there remains a need for integrated software frameworks that combine acquisition and analysis. Here we present deepthought, a framework built on domain-driven design principles that unifies microscope control and data analysis through a common domain language. This framework enables automated high-throughput imaging with real-time analysis capabilities, demonstrated through studies of DNA damage responses in live cells. By implementing deepthought on a standard wide-field microscope, we achieved sample sizes exceeding 10,000 cells per condition and identified rare cellular subpopulations, capabilities typically limited to specialized high-content systems. Our approach provides a foundation for developing context-aware microscopy software that can dynamically adjust experimental parameters based on real-time analysis of biological phenomena.

microscopy, software, design, automation, online-analysis, cell biology, DNA damage responses

Correspondence: *pskesavan@tifrh.res.in*

Introduction

Microscope systems have traditionally separated data acquisition and analysis, creating a fundamental operational challenge that limits the potential of biological imaging [Scherf and Huisken, 2015]. This artificial separation has been recognized as a problem since the earliest computer-controlled microscopes in the mid-20th century [Wald, 1966, Herron et al., 1972, Brenner et al., 1976], with various conceptual solutions proposed over decades. Yet despite widespread acknowledgment of these limitations, the pattern of disconnected acquisition and analysis persists in modern microscopy.

This persistence raises an important question: why, despite clear conceptual solutions, has integrated microscopy not been widely adopted? Recent attempts to bridge this gap have produced diverse approaches, from event-driven architectures for capturing rare biological events [Mahecic et al., 2022] to middleware platforms enabling distributed workflows [Roos et al., 2024] and modular frameworks for specific microscopy modalities [Marin et al., 2024]. Despite these advances, widespread adoption remains limited. We hypothesize that the core issue is democratization. While commercial computing systems have become increasingly accessible through dramatic improvements in usability, cost, and availability, the design of sophisticated microscopy software remains challenging. The barriers to adopting feedback microscopy techniques—recently rebranded as "smart microscopy"—stem largely from this democratization gap, particularly the lack of easily designable control software.

An additional challenge emerges from the nature of democratization itself. Each wave of technological democratization has produced more user-friendly solutions, but these often take the form of deeply integrated packages that reach end users with limited scope for multilevel modifications. Commercial microscopy systems may offer hardware flexibility and application diversity, but their fundamental design reflects the commercial motivations of manufacturers rather than the spirit of open scientific progress. This creates a paradoxical situation where increasing accessibility comes at the cost of decreasing adaptability at the system level. Early attempts at integration like Acquiarium [Matula et al., 2009] demonstrated the potential of unified acquisition and analysis but were limited by technology constraints of their time. Modern approaches have evolved to address these limitations through varying architectural patterns - from neural network-driven smart acquisition [Mahecic et al., 2022] to containerized microservices [Roos et al., 2024] - yet each introduces its own complexity and resource demands.

This separation creates significant operational challenges: scanning samples visually to identify regions of interest is both error-prone and time-consuming for human operators. Moreover, manual scanning exposes samples to excessive light, depleting the photon budget and potentially creating destructive phototoxicity artifacts in living samples [Ge et al., 2013].

Our approach addresses these fundamental problems through several guiding principles. First, we prioritize simplicity, avoiding unnecessary complexity that distracts from the biologist's primary goal of discovery. The microscope should serve as a means to scientific ends rather than becoming an end itself [Ian, 1922]. Second, we leverage mature, open-source tools like micro-manager [Edelstein et al., 2014] to create clean patterns that are intuitive to read, use, and adapt. This prevents redundant development while ensuring accessi-

bility. Third, the system must be as generalizable as possible, with clearly defined inputs and outputs that enable straightforward testing across diverse microscope configurations.

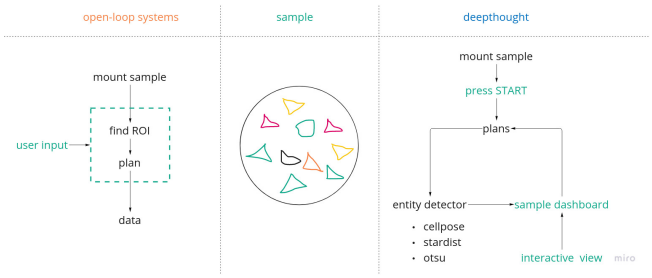

Fig. 1. Difference between open-loop and closed-loop software workflows for imaging a sample. In the open-loop system (right), after mounting a sample (centre), the user performs tasks with software, which includes finding the relevant regions of interest and defining an experimental plan from predefined experimentation patterns. Upon receiving a configuration, the system outputs raw data based on the experimental plan, which is the end point of such a system. Using deepthought, the sample is mounted by the user, and after that, a plan is executed, which involves a grid search for entities using detectors, and displays the quantitative properties of the sample in a dashboard. The quantitative data can be used as feedback to the experimental plans, which makes this a closed-loop system.

At the foundation of our solution is domain-driven design [Evans and Evans, 2004], which clearly demarcates process boundaries using appropriate layers of abstraction. This creates a system that is conceptually sound from multiple perspectives—whether viewed by a biologist, microscopist, or systems designer. By presenting these patterns in their most minimal form, we enable users to intuitively introduce complexity where needed for specific applications.

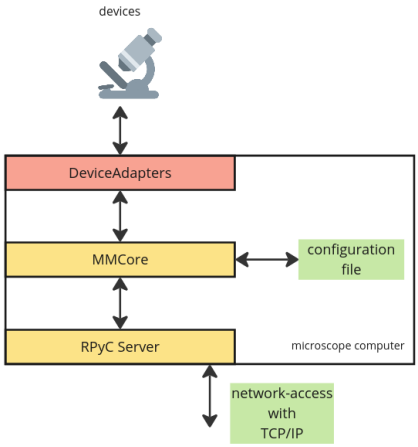

Fig. 2. The system architecture of the device control server. Devices are connected to the hardware ports in the computer by cables. In the microscope computer, Device Adapters that are written in C++, bundled with micro-manager, manage the communication with the devices, and MMCore, which is the abstract model of a microscope as defined by micro-manager, is exposed to clients through TCP/IP. MMCore requires a configuration file with the various devices defined.

To address these limitations, we developed a network-enabled device control architecture that serves as the foundation for automated microscopy (Fig. 2). This system translates high-level experimental commands into coordinated device operations through micro-manager device adapters, building upon established principles of domain-driven design to enable robust error handling and system stability.

The traditional microscopy workflow represents an open-loop system, where image acquisition and analysis are entirely separated (Fig. 1). Raw data is typically stored in proprietary formats on the acquisition computer before being transferred to analysis workstations [Haase et al., 2022]. This workflow has several major drawbacks: it requires multiple disk write operations, prevents real-time analysis that could guide experimental decisions, and makes it challenging to capture rare cellular events without extensive oversampling. When errors are detected during post-acquisition analysis, it is often too late to adjust the imaging strategy or revisit the sample [Dhiman et al., 2022]. Recent advances in data-driven microscopy have demonstrated how real-time analysis can enable targeted imaging of specific phenotypes [André et al., 2023], but these solutions often require specialized hardware configurations or complex setup procedures that limit their widespread adoption.

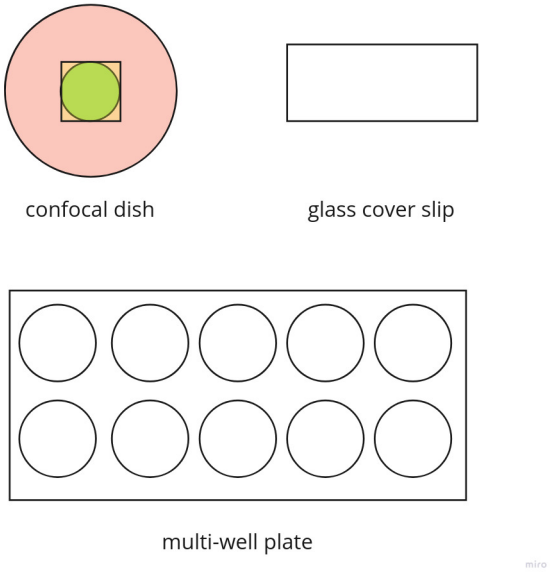

Fig. 3. Top view of various sample forms commonly used in microscopes today. All samples have a physical form in 2D, such as a dish, slide or a large plate with multiple dishes. The top left features a confocal dish with a glass coverslip (yellow square) on the bottom, providing a glass imaging surface (green) suitable for optical imaging. Other structural forms commonly used in imaging are also shown here, such as a rectangular glass coverslip (top right) and a multi-well plate with many isolated wells.

To enable more sophisticated experimental workflows, microscope software must account for the physical constraints of different sample types. Common sample formats like confocal dishes, glass slides, and multi-well plates each present unique geometric considerations that affect imaging strategy (Fig. 3). Understanding these physical parameters is essential for efficient automated scanning and focus maintenance [Patel et al., 2015].

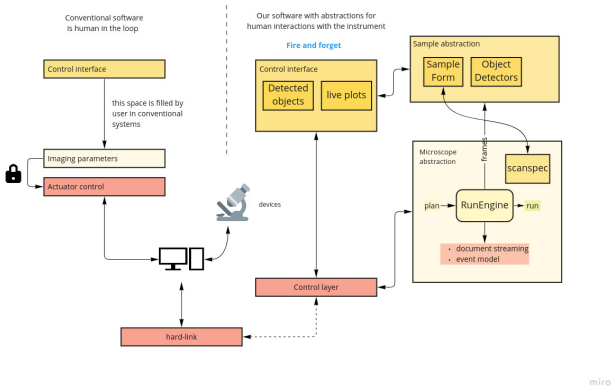

Fig. 4. Software architecture of traditional systems, compared with deepthought, the closed-loop multi-layered system of modular planning, and sample abstraction. The device is connected physically to a computer, which acts as a control hub. In traditional systems, the entire stack of the microscope control software is installed on this computer. The software has a control interface, which acts as a graphical interface for the user to input imaging parameters, translating into actuator control. In the case of deepthought, the device control computer is running the hard-link server, a wrapper for a micro-manager and a network server that receives command messages from a client.

We hypothesized that redesigning microscope software architecture as a modular, closed-loop system could unlock new experimental capabilities from existing hardware. Our solution, implemented as the deepthought framework, integrates acquisition with analysis and introduces an event-driven model for microscope control (Fig. 4). This architecture separates device control from experimental logic, following recent trends in scientific software design [Allan et al., 2019] while enabling real-time analysis to guide data collection.

The deepthought framework introduces several key abstractions that facilitate automated microscopy, inspired by successful implementations in high-content screening systems [Stossi et al., 2022, Perlman et al., 2004]. Frame objects encapsulate imaging data as it is generated, enabling real-time processing and feature detection. Albums collect and organize detected objects, providing a structured way to track experimental observations, similar to approaches used in automated cellular phenotyping [Kondo et al., 2021].

This design transforms the microscope from a passive data collection tool into an intelligent imaging system that can autonomously identify and characterize biological phenomena. We demonstrate the utility of this approach through studies of DNA damage responses, where automated imaging reveals population heterogeneity and rare cellular events that would be difficult to capture through conventional methods [Kesavan et al., 2020].

In this paper, we present the implementation of deepthought and demonstrate its capabilities through several challenging applications in DNA damage response studies. Our results show that this architecture can transform a standard motorized microscope into a high-throughput imaging platform capable of generating datasets comparable to specialized screening systems, while maintaining the flexibility to investigate complex biological phenomena [Mazumder et al., 2013].

Results

High-throughput mapping of fixed and live cells using deepthought. The development of deepthought enabled us to investigate cellular heterogeneity in DNA damage responses through automated imaging of large cell populations. We first validated the system's capability to acquire and analyze immunofluorescence data at scale, focusing on key DNA damage response markers.

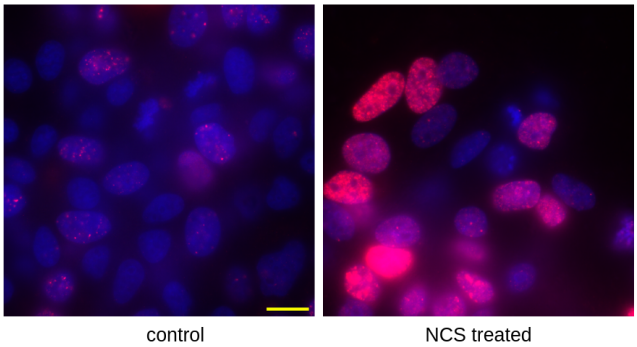

Fig. 5. Representative image of immuno-fluorescence against γH2AX (red) in HeLa cells from a high-throughput dataset acquired with deepthought. Nuclei are stained with DAPI (blue). Cells were damaged with neocarzinostatin (NCS) for 5 minutes, followed by 15 minutes of recovery, and fixed and stained for γH2AX. Treated cells show increased staining of the antibody. The scale bar corresponds to 15 μm.

Automated acquisition reveals population-level DNA damage responses. Cells were treated with neocarzinostatin (NCS), a radiomimetic DNA damage agent, and analyzed for γH2AX and phosphorylated Chk1 expression through immunofluorescence (Fig. 5). γH2AX, the phosphorylated form of histone variant H2A.X, serves as a general marker for DNA damage, while phosphorylated Chk1 indicates activation of cell cycle checkpoint responses. The system automatically imaged and analyzed 22,000 cells (11,000 each for control and treatment conditions) without manual intervention.

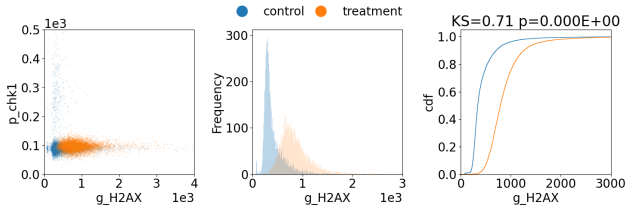

Fig. 6. Automated immuno-fluorescence imaging against γH2AX and phosphorylated Chk1 with a sample size of N=11000 for control and treated each. HeLa cells are treated with NCS as described in Fig. 5. On the left is a scatter plot with the mean level of γH2AX on the x-axis and the mean level of phosphorylated Chk1 on the y-axis, and each data point represents a cell. It can be observed that the mean levels of γH2AX in treated cells are shifted to the right (positive increase in mean) without any shift in the levels of phosphorylated Chk1. The increase in the levels of γH2AX can be seen in the histogram (center), and the differences between the distribution are quantifiable with the cumulative density function (CDF) (right).

Analysis of this dataset revealed that NCS treatment induced a clear increase in mean γH2AX levels without significantly affecting phosphorylated Chk1 levels (Fig. 6). The large sample size enabled fine resolution of the response distribution, providing a comprehensive view of population hetero-

geneity that would be challenging to achieve through conventional microscopy approaches.

Increasing sample size reveals distinct cellular subpopulations. To further investigate population heterogeneity, we treated cells with 0.02% methyl methanesulfonate (MMS), which induces base excision repair through DNA methylation. By analyzing γH2AX and phosphorylated Chk1 levels across different sample sizes (N = 30, 300, 3000, and 12,000 cells), we demonstrated how increased sampling progressively revealed distinct cellular subpopulations (Fig. 7). These subpopulations, characterized by differential phosphorylated Chk1 responses, were only reliably detected with sample sizes above 3,000 cells.

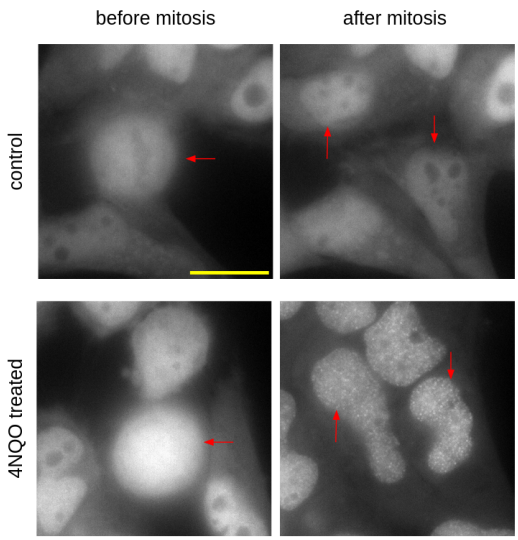

Fig. 8. Automated microscopy identifies rare subpopulations of G1 HeLa cells expressing PCNA chromobody undergoing repair sustained before cell division. Many fields of cells were imaged for 24 hours in control and treatment conditions. Both data sets selected cells with the morphology of G2 cells manually. In control conditions, G1 cells post mitosis show diffused PCNA signal, whereas 4NQO treated (1μg/ml for 15 minutes, followed by PBS wash) G1 cells show punctated PCNA, indicating ongoing repair from damage sustained in the parent cell and carried forward through mitosis. The arrows mark parent (left) and daughter cells (right). The scale bar corresponds to 15 μm.

Live cell imaging identifies rare cellular phenomena. The success in fixed-cell imaging prompted us to explore the system's capabilities in live-cell applications. Using HeLa cells expressing PCNA-chromobody, we tracked DNA damage responses in asynchronous cell populations over 24 hours. This approach eliminated the need for chemical synchronization, allowing observation of natural cell cycle progression and damage responses.

By imaging many fields of view over extended periods, we identified rare cellular events that would be difficult to capture through conventional methods. Notably, we observed the transmission of DNA damage repair foci from parent to daughter cells through mitosis (Fig. 8). In control conditions, G1 cells post-mitosis displayed diffuse PCNA signal, while cells treated with 4NQO showed punctate PCNA patterns in G1 daughter cells, indicating inheritance of active repair sites.

This observation of repair foci inheritance through cell division represents a phenomenon that would be challenging to detect without the high-throughput capabilities of our system. The ability to track such events in unperturbed, asynchronous cultures provides insights that might be masked by traditional synchronization approaches.

Through these applications, we demonstrate that deepthought can transform a standard wide-field microscope into a high-throughput imaging platform capable of revealing both population-level trends and rare cellular behaviors. The integration of acquisition and analysis enables rapid data collection while maintaining the ability to detect and validate significant biological phenomena in real-time.

Discussion

The integration of acquisition and analysis in microscopy software represents a significant step toward more efficient and insightful biological imaging. Through the development of deepthought, we have demonstrated how domain-driven design principles can create a robust framework for automated microscopy that enhances experimental capabilities without requiring specialized hardware.

Our approach to microscope software architecture addresses several fundamental challenges in contemporary microscopy. At the most basic level, a microscope can be abstracted as a collection of motors and detectors, where motors control components like filter wheels and stage position, while detectors include cameras and other sensing devices. While this implementation uses micro-manager for device control, the architecture's modular nature means it can accommodate any abstract imaging and motor devices with minimal modifications, making it adaptable across different experimental contexts.

The separation of device control into a network-accessible server layer represents a significant advance in microscope software design. This architecture provides several advantages: it isolates client application logic from device control, simplifies debugging, and prevents system-wide failures due to client errors. Furthermore, the network-enabled approach allows for cross-platform operation, with clients running on any operating system that supports Python.

The real-time integration of acquisition and analysis addresses a critical limitation of traditional microscopy workflows. In conventional systems, the disconnect between imaging and analysis creates a temporal gap that can lead to missed opportunities for experimental optimization. Our closed-loop system enables immediate validation of image quality and experimental parameters, allowing for rapid adjustment of acquisition strategies based on preliminary findings.

The application of deepthought to DNA damage response studies demonstrates its practical utility in addressing complex biological questions. The ability to automatically image and analyze over 10,000 cells per condition using standard microscopy equipment approaches the capabilities of specialized high-content screening systems. This high throughput revealed population heterogeneity and rare cellular events

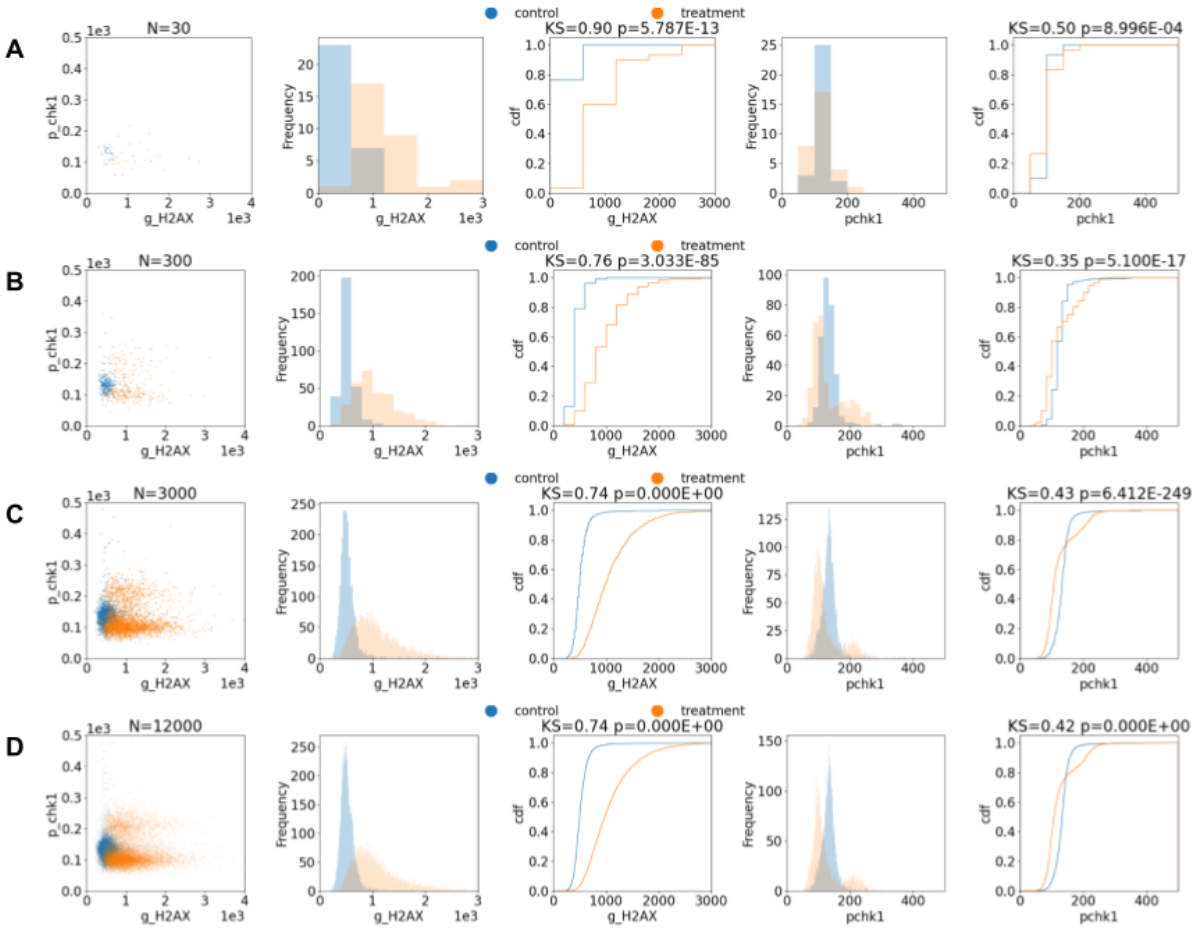

Fig. 7. Automated immuno-fluorescence imaging against γH2AX and phosphorylated Chk1 in HeLa cells for increasing N in control and treatment of 0.02% MMS (5 minutes, followed by 15 minutes recovery) show a subpopulation of treated cells. Scatter plot of γH2AX against phosphorylated Chk1, histogram and cumulative density function of control and treatment levels of γH2AX and phosphorylated Chk1, for increasing N of **(A)** 30, **(B)** 300, **(C)** 3000 and **(D)** 12,000 cells are plotted.

that might be missed in smaller-scale studies, such as the inheritance of repair foci through cell division.

Perhaps most significantly, this work establishes a foundation for developing truly adaptive microscopy systems. By combining domain-driven design with real-time analysis capabilities, we create the possibility for microscopes that can autonomously adjust their acquisition parameters based on the biological phenomena they observe. This capability could be particularly valuable in studying dynamic cellular processes where experimental conditions may need to be modified in response to observed behaviors.

The open-source nature of deepthought (available at https://github.com/ndsystems/deepthought) ensures that this framework can be adapted and extended by the broader scientific community. While our implementation focused on DNA damage responses, the underlying architecture could be applied to various biological imaging contexts, from developmental biology to neuroscience.

Looking forward, this approach to microscope software design opens several promising avenues for future development. Integration with machine learning algorithms could further enhance the system's ability to identify and respond to biological events of interest. Additionally, the network-enabled architecture could facilitate the development of distributed imaging systems where multiple microscopes collaborate to build comprehensive datasets.

In conclusion, deepthought demonstrates how modern software design principles can enhance biological imaging capabilities. By bridging the gap between acquisition and analysis, we create new opportunities for discovery while making high-throughput microscopy more accessible to the broader research community. This work provides a template for developing next-generation microscopy tools that are both more capable and more user-friendly than traditional approaches.

Methods

Cell culture and maintenance. HeLa cells and HeLa cells stably expressing PCNA-chromobody were cultured in DMEM/F12 supplemented with 10% FBS (Gibco, 16000-044) and 1% PenStrep-glutamine (Gibco, 10378-016). Cells were maintained in T-25 flasks (Corning) at 37°C with 5% CO^2 in a humidified incubator (Eppendorf Galaxy 170S). For imaging experiments, cells were plated on glass-bottom dishes (Genetix, 200350) 24 hours before experimentation.

DNA damage treatments. For DNA double-strand break induction, cells were treated with neocarzinostatin (NCS, Sigma, N9162) at 1 µg/ml for 5 minutes followed by a 15-

minute recovery period. Base excision repair was induced using methyl methanesulfonate (MMS, Sigma, 129925) at 0.02% concentration for 5 minutes followed by 15 minutes of recovery. For UV-mimetic damage, cells expressing PCNA-chromobody were treated with 4-Nitroquinoline 1-oxide (4NQO, Sigma) at 1 µg/ml for 15 minutes, followed by PBS washes. Live-cell imaging was performed in FluoroBrite medium (Gibco, A18967-01) supplemented with 10% FBS and 1% PenStrep-glutamine.

Immunofluorescence. Cells were fixed with 4% paraformaldehyde (Sigma P6148) in PBS for 10 minutes at room temperature. After two PBS washes, cells were permeabilized using 0.3% Triton X-100 (Sigma, T8787) in PBS for 10 minutes. Following permeabilization and two PBS washes, samples were blocked with 5% BSA (Himedia TC545) in PBS for one hour. Primary antibodies were diluted in blocking solution and applied overnight at 4°C. After three PBS washes, samples were incubated with secondary antibodies in blocking solution for 2 hours at room temperature. Following three additional PBS washes, nuclei were stained with DAPI (1 µg/ml in PBS) for 10 minutes. Samples were maintained in PBS for imaging unless otherwise specified.

Microscopy and image acquisition. Images were acquired using a 60x objective on an Olympus IX83 motorized inverted microscope (Tokyo, Japan) equipped with an Andor Zyla 4.2 scientific CMOS camera. The microscope was controlled through the hard-link server, which provides network-accessible control of microscope components through micro-manager device adapters. The system was configured using standard micro-manager device configuration files, with additional parameters defined through the deepthought framework.
Live-cell imaging was performed using an environmental chamber by Okolab UNO (Naples, Italy) maintaining 37°C, 5% CO^2, and humidity. Time-lapse sequences were acquired at 20-minute intervals for 24 hours, with automated focus maintenance between timepoints. Multiple positions were imaged in parallel to maximize data collection while minimizing photobleaching and phototoxicity.

Image analysis and data processing. Image analysis was performed in real-time using the deepthought framework. For fixed-cell analysis, nuclear regions were identified from DAPI images using automated segmentation algorithms. Intensity measurements for γH2AX and phosphorylated Chk1 were extracted from each nuclear region, with local background subtraction applied to correct for imaging artifacts.
For live-cell experiments, PCNA-chromobody signals were analyzed to track DNA replication patterns and repair foci. Cell tracking was performed using nuclear signals, with automated detection of mitotic events based on characteristic changes in nuclear morphology. Data analysis was performed using custom Python scripts within the deepthought framework, with statistical analyses performed using standard scientific Python libraries.

Statistical analysis. Statistical significance was assessed using appropriate statistical tests based on data distributions. For comparisons between control and treated populations, Kolmogorov-Smirnov tests were used to evaluate differences in distributions. Sample sizes were determined based on preliminary experiments to ensure adequate statistical power for detecting biologically relevant differences.

Software availability. The source code for deepthought and associated analysis tools is freely available at https://github.com/ndsystems/deepthought. The repository includes detailed documentation, installation instructions, and example configurations for common experimental scenarios.

Acknowledgements

We thank the members of the Mazumder lab at TIFR Hyderabad for their valuable discussions and support throughout this project. We are grateful to the Imaging and Flow Cytometry Facility (supported by DAE project # RTI 4007) at TIFR Hyderabad for their technical assistance. Special thanks to Subindev Devadasan and Jensun Ravichandran for providing important inputs during software development. We also thank the bluesky community for their pioneering work in scientific data acquisition software design that influenced this project.

References

[lan, 1922] (1922). The microscopist and his tools. *The Lancet*, 200(5178):1135.

[Allan et al., 2019] Allan, D., Caswell, T., Campbell, S., and Rakitin, M. (2019). Bluesky's Ahead: A Multi-Facility Collaboration for an a la Carte Software Project for Data Acquisition and Management. *Synchrotron Radiation News*, 32(3):19–22.

[André et al., 2023] André, O., Ahnlide, J. K., Norlin, N., Swaminathan, V., and Nordenfelt, P. (2023). Data-driven microscopy allows for automated context-specific acquisition of high-fidelity image data. *Cell reports methods*, 3(3).

[Brenner et al., 1976] Brenner, J. F., Dew, B. S., Horton, J. B., King, T., Neurath, P. W., and Selles, W. D. (1976). An automated microscope for cytologic research a preliminary evaluation. *The journal of histochemistry and cytochemistry : official journal of the Histochemistry Society*, 24:100 – 111.

[Dhiman et al., 2022] Dhiman, S., Andrian, T., Gonzalez, B. S., Tholen, M. M. E., Wang, Y., and Albertazzi, L. (2022). Can super-resolution microscopy become a standard characterization technique for materials chemistry? *Chem. Sci.*, pages –.

[Edelstein et al., 2014] Edelstein, A. D., Tsuchida, M. A., Amodaj, N., Pinkard, H., Vale, R. D., and Stuurman, N.

(2014). Advanced methods of microscope control using μmanager software. *J. Biol. Meth.*, 1(2).

[Evans and Evans, 2004] Evans, E. and Evans, E. J. (2004). *Domain-driven design: tackling complexity in the heart of software*. Addison-Wesley Professional.

[Ge et al., 2013] Ge, J., Wood, D. K., Weingeist, D. M., Prasongtanakij, S., Navasumrit, P., Ruchirawat, M., and Engelward, B. P. (2013). Standard fluorescent imaging of live cells is highly genotoxic. *Cytom Part A*, 83(6):552–560.

[Haase et al., 2022] Haase, R., Fazeli, E., Legland, D., Doube, M., Culley, S., Belevich, I., Jokitalo, E., Schorb, M., Klemm, A., and Tischer, C. (2022). A hitchhiker's guide through the bio-image analysis software universe. *FEBS letters*.

[Herron et al., 1972] Herron, J. M., Ranshaw, R. W., Castle, J., and Wald, N. (1972). Automatic microscopy for mitotic cell location. *Computers in biology and medicine*, 2 2:129–35.

[Kesavan et al., 2020] Kesavan, P., Bohra, D., Roy, S., and Mazumder, A. (2020). Monitoring global changes in chromatin compaction states upon localized DNA damage with tools of fluorescence anisotropy. *Mol. Biol. Cell*, 31(13):1403–1410.

[Kondo et al., 2021] Kondo, H., Ratcliffe, C. D., Hooper, S., Ellis, J., MacRae, J. I., Hennequart, M., Dunsby, C. W., Anderson, K. I., and Sahai, E. (2021). Single-cell resolved imaging reveals intra-tumor heterogeneity in glycolysis, transitions between metabolic states, and their regulatory mechanisms. *Cell reports*, 34(7):108750.

[Mahecic et al., 2022] Mahecic, D., Stepp, W. L., Zhang, C., Griffié, J., Weigert, M., and Manley, S. (2022). Event-driven acquisition for content-enriched microscopy. *Nature methods*, 19(10):1262–1267.

[Marin et al., 2024] Marin, Z., Wang, X., Collison, D. W., McFadden, C., Lin, J., Borges, H. M., Chen, B., Mehra, D., Shen, Q., Gałecki, S., et al. (2024). navigate: an open-source platform for smart light-sheet microscopy. *Nature methods*, 21(11):1967–1969.

[Matula et al., 2009] Matula, P., Maska, M., Danek, O., Matula, P., and Kozubek, M. (2009). Acquiarium: free software for the acquisition and analysis of 3d images of cells in fluorescence microscopy. In *2009 IEEE International Symposium on Biomedical Imaging: From Nano to Macro*, pages 1138–1141. IEEE.

[Mazumder et al., 2013] Mazumder, A., Pesudo, L. Q., McRee, S., Bathe, M., and Samson, L. D. (2013). Genome-wide single-cell-level screen for protein abundance and localization changes in response to dna damage in s. cerevisiae. *Nucleic acids research*, 41(20):9310–9324.

[Patel et al., 2015] Patel, T. P., Man, K., Firestein, B. L., and Meaney, D. F. (2015). Automated quantification of neuronal networks and single-cell calcium dynamics using calcium imaging. *Journal of neuroscience methods*, 243:26–38.

[Perlman et al., 2004] Perlman, Z. E., Slack, M. D., Feng, Y., Mitchison, T. J., Wu, L. F., and Altschuler, S. J. (2004). Multidimensional drug profiling by automated microscopy. *Science*, 306(5699):1194–1198.

[Roos et al., 2024] Roos, J., Bancelin, S., Delaire, T., Wilhelmi, A., Levet, F., Engelhardt, M., Viasnoff, V., Galland, R., Nägerl, U. V., and Sibarita, J.-B. (2024). Arkitekt: streaming analysis and real-time workflows for microscopy. *Nature methods*, 21(10):1884–1894.

[Scherf and Huisken, 2015] Scherf, N. and Huisken, J. (2015). The smart and gentle microscope. *Nat. Biotechnol.*, 33(8):815–818.

[Stossi et al., 2022] Stossi, F., Singh, P. K., Mistry, R. M., Johnson, H. L., Dandekar, R. D., Mancini, M. G., Szafran, A. T., Rao, A. U., and Mancini, M. A. (2022). Quality control for single cell imaging analytics using endocrine disruptor-induced changes in estrogen receptor expression. *Environmental health perspectives*, 130(2):027008.

[Wald, 1966] Wald, N. (1966). Contract to extend the usefullness of cytogenetic methodology as a research technique and as a biomedical monitoring procedure quarterly progress report 1 jan.-30 jun. 1966. Technical report.